

# Optical and Scintillation Properties of Eu-doped CsBr–BaBr<sub>2</sub>–ZnBr<sub>2</sub> Glasses

Hiromi Kimura,\* Takumi Kato, Daisuke Nakauchi,  
Noriaki Kawaguchi, and Takayuki Yanagida

Division of Materials Science, Nara Institute of Science and Technology (NAIST),  
8916-5 Takayama-cho, Ikoma-shi, Nara 630-0192, Japan

(Received October 12, 2021; accepted October 26, 2021)

**Keywords:** photoluminescence, scintillation, ZnBr<sub>2</sub>-based glass

20CsBr–20BaBr<sub>2</sub>–60ZnBr<sub>2</sub> glasses doped with various concentrations of Eu (0.01, 0.05, 0.1, and 0.5%) were synthesized by the melt-quenching method, and their optical and scintillation properties were investigated. In the photoluminescence (PL) and X-ray-induced scintillation spectra of all the prepared glasses, the emission band around 415 nm due to the 5d–4f transitions of Eu<sup>2+</sup> was observed. In the scintillation spectrum, the 0.5% Eu-doped glass showed sharp emission peaks at 590 and 610 nm, which have a typical spectral shape for the 4f–4f transitions of Eu<sup>3+</sup>. Under <sup>241</sup>Am  $\alpha$ -ray irradiation, the light yields of 0.01 and 0.05% Eu-doped glasses were 75 and 100 ph/5.5 MeV- $\alpha$ , respectively.

## 1. Introduction

In radiation measurements, scintillation detectors are often used in various fields, including medicine,<sup>(1)</sup> security,<sup>(2)</sup> well logging,<sup>(3,4)</sup> environmental monitoring,<sup>(5,6)</sup> and high-energy physics.<sup>(7)</sup> The scintillation detectors consist of scintillators, which are materials that immediately convert high-energy ionizing radiation such as X- or  $\gamma$ -rays to low-energy photons, and photodetectors including photomultiplier tubes or photodiodes.<sup>(8)</sup> Since the performance of scintillation detectors mainly depends on the scintillation properties and chemical composition of scintillators, the scintillation properties of many materials have been investigated.<sup>(9–18)</sup> The required properties of scintillators for X- and  $\gamma$ -ray detection are a large effective atomic number ( $Z_{\text{eff}}$ ), a short decay time, a high light yield, and a low spatial resolution.<sup>(19)</sup> To date, the material forms of commercial scintillators for X- and  $\gamma$ -ray detection have used mainly single crystals because of their high density and optical qualities. However, single crystals have some disadvantages, including high cost and difficulty in increasing their sizes.<sup>(20)</sup> From the viewpoint of industry, glasses have many merits such as low cost, high productive efficiency, and flexibility of chemical composition.<sup>(21,22)</sup> However, the commercial scintillator in the form of glasses is only Li glass (GS20, Saint-Gobain) for neutron detectors,

---

\*Corresponding author: e-mail: [kimura.hiromi.kf1@ms.naist.jp](mailto:kimura.hiromi.kf1@ms.naist.jp)  
<https://doi.org/10.18494/SAM3687>

which consists of light elements.<sup>(23,24)</sup> Thus, the development of glass scintillators composed of heavy elements for X- and  $\gamma$ -ray detection has been expected.

To date, the scintillation properties of oxide glasses have been studied by many researchers,<sup>(25–31)</sup> whereas those of non-oxide glasses have not been studied extensively. Recently, there have been a few reports on the scintillation properties of non-oxide glasses such as  $AEF_2-Al_2O_3-B_2O_3$  ( $AE = Ca, Sr, Ba$ ),<sup>(32–34)</sup>  $BaF_2-Gd_2O_3-Lu_2O_3-B_2O_3-SiO_2$ ,<sup>(35)</sup>  $CeCl_3-CsCl-CsPO_3-Al(PO_3)_3$ ,<sup>(36)</sup> and  $CsCl-BaCl_2-ZnCl_2$ .<sup>(37,38)</sup> In particular,  $AEF_2-Al_2O_3-B_2O_3$  shows higher quantum yields (>80%) and light yields (~1800 ph/MeV) than the reported oxide glasses. Thus, non-oxide glasses as scintillators can be considered as promising materials.

In this study, we focused on bromide glasses. Among the reported bromide glasses, the optical properties of  $ZnBr_2$ -based glasses were studied, whereas there are no reports on the scintillation properties of bromide glasses.<sup>(39,40)</sup> Thus, we investigated the optical and scintillation properties of the Eu-doped  $20CsBr-20BaBr_2-60ZnBr_2$  glasses and compared them with those of the Eu-doped  $20CsCl-20BaCl_2-60ZnCl_2$  glasses.

## 2. Materials and Methods

$20CsBr-20BaBr_2-60ZnBr_2$  glasses doped with various concentrations of Eu (0.01, 0.05, 0.1, and 0.5%) were synthesized by the melt-quenching method. Powders of CsBr (99.99%, Furuuchi Chemical),  $BaBr_2$  (99.9%, Furuuchi Chemical),  $ZnBr_2$  (99.99%, High Purity Chemicals), and  $EuBr_3 \cdot xH_2O$  (99.99%, Sigma-Aldrich) were mixed at a molar ratio of 20:20:60: $x$  ( $x = 0.01, 0.05, 0.1, \text{ and } 0.5$ ). The mixed powders were loaded in a quartz tube and then dried at 300 °C for 3 h under vacuum. The dried powders were enclosed in a vacuum-sealed quartz ampule and melted at 700 °C for 1 h using an electric furnace. To rapidly cool the melts, the enclosed ampule was immersed in water at room temperature. To investigate the optical and scintillation properties of the prepared glasses, these quartz ampules were crushed, and the surfaces of the obtained glasses were polished using various sandpapers (600–3000 grits) and characterized by the following procedures.

As the optical properties, the diffuse transmittance spectra, photoluminescence (PL) excitation/emission maps, and PL decay curves were measured using a spectrophotometer (Shimadzu, SolidSpec-3700), Quantaurus- $QY$  (Hamamatsu Photonics, C11347), and Quantaurus- $\tau$  (Hamamatsu Photonics, C11367), respectively. In addition, the PL  $QY$  was obtained using the Quantaurus- $QY$ .

As the scintillation properties, the X-ray-induced scintillation spectra and decay curves were measured using an original setup.<sup>(41,42)</sup> To evaluate the light yields, the pulse height spectra were measured using a custom-made setup reported previously.<sup>(41)</sup>

## 3. Results and Discussion

Figure 1 shows photographs of 0.01, 0.05, 0.1, and 0.5% Eu-doped  $20CsBr-20BaBr_2-60ZnBr_2$  glasses under room light. The thickness of all the glasses was fixed at 1.0 mm. Although all the glasses looked transparent, the surfaces became slightly cloudy after a few minutes because the prepared glasses are deliquescent.

Figure 2 shows the diffuse transmission spectra of Eu-doped  $20\text{CsBr}-20\text{BaBr}_2-60\text{ZnBr}_2$  glasses. The transmittance of all the glasses was  $\sim 50\%$  in the wavelength range of 400–800 nm. In all the glasses, the absorption band around 350 nm was observed, and the band expanded to a longer wavelength with increasing concentrations of Eu. Since the absorption band around 350 nm was also confirmed with previous reports on the Eu-doped glasses, the origin was considered to be the  $4f-5d$  transitions of  $\text{Eu}^{2+}$ .<sup>(38,43,44)</sup>

Figure 3 shows PL excitation and emission maps of 0.1% Eu-doped  $20\text{CsBr}-20\text{BaBr}_2-60\text{ZnBr}_2$  glass as a representative. Under excitation wavelengths of 280–380 nm, the emission band was observed at around 415 nm. The excitation and emission spectral shapes of all the Eu-doped glasses were similar to that of the 0.1% Eu-doped glass, which was consistent with previous studies.<sup>(38,45)</sup> The PL decay curves of Eu-doped  $20\text{CsBr}-20\text{BaBr}_2-60\text{ZnBr}_2$  glasses at the monitoring wavelength of 415 nm and excitation wavelength of 340 nm are shown in Fig. 4. All the decay curves were well approximated by the sum of two exponential decay functions, and the lifetimes of 46–54 ns and 0.25–0.27  $\mu\text{s}$  were obtained. The faster components were due to the instrumental response function (IRF), and the slower

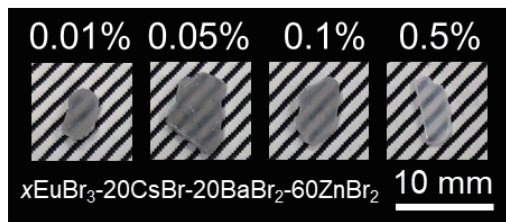


Fig. 1. Photographs of Eu-doped  $20\text{CsBr}-20\text{BaBr}_2-60\text{ZnBr}_2$  glasses under room light.

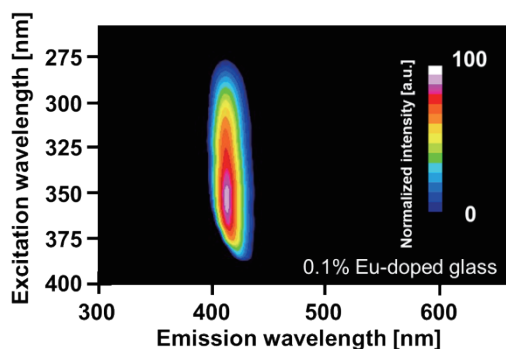


Fig. 3. (Color online) PL excitation and emission maps of 0.1% Eu-doped  $20\text{CsBr}-20\text{BaBr}_2-60\text{ZnBr}_2$  glass.

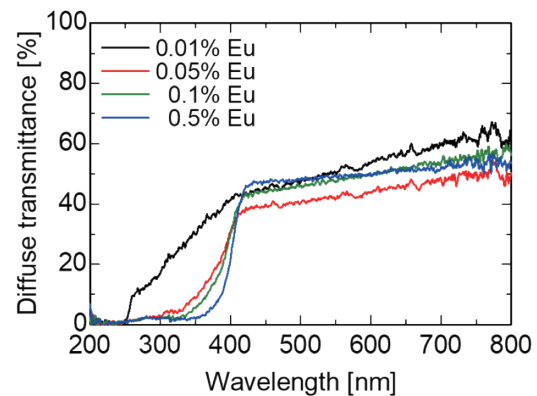


Fig. 2. (Color online) Diffuse transmission spectra of Eu-doped  $20\text{CsBr}-20\text{BaBr}_2-60\text{ZnBr}_2$  glasses.

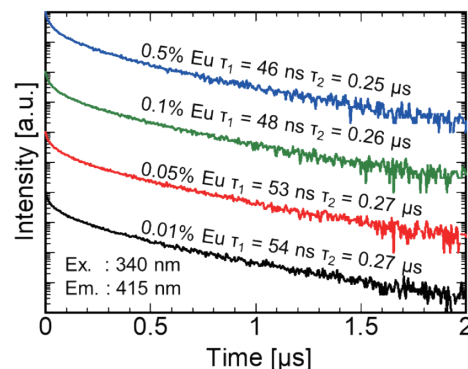


Fig. 4. (Color online) PL decay curves of Eu-doped  $20\text{CsBr}-20\text{BaBr}_2-60\text{ZnBr}_2$  glasses at monitoring wavelength of 415 nm and excitation wavelength of 340 nm.

components were typical values for the 5d–4f transitions of  $\text{Eu}^{2+}$ .<sup>(38,45,46)</sup> Judging from the excitation and emission wavelengths and lifetimes, the origin of the emission at around 415 nm was due to the 5d–4f transitions of  $\text{Eu}^{2+}$ . In contrast, the emission due to  $\text{Eu}^{3+}$  was not confirmed despite doping  $\text{Eu}^{3+}$  ions as the starting powder. In previous studies, the  $\text{Eu}^{3+}$  ions were reduced to  $\text{Eu}^{2+}$  ions when some glasses such as borates, phosphates, and silicates were prepared at high temperature.<sup>(45,47–49)</sup> Therefore, it is considered that the same phenomenon occurred in the Eu-doped  $\text{CsBr–BaBr}_2\text{–ZnBr}_2$  glasses. The PL  $QY$  values of 0.01, 0.05, 0.1, and 0.5% Eu-doped glasses were 2.1, 1.9, 1.8, and 6.4%, respectively, which were similar to that of Eu-doped  $20\text{CsCl–}20\text{BaCl}_2\text{–}60\text{ZnCl}_2$  glasses ( $\sim 3.3\%$ ).<sup>(38)</sup>

The X-ray-induced scintillation spectra of Eu-doped  $20\text{CsBr–}20\text{BaBr}_2\text{–}60\text{ZnBr}_2$  glasses are presented in Fig. 5. All the glasses showed the main emission peak at around 415 nm. Since the spectral features were consistent with the PL result, the emission peak at around 415 nm was due to the 5d–4f transitions of  $\text{Eu}^{2+}$ . In the 0.5% Eu-doped glass, the sharp emission peaks at 590 and 610 nm were observed, which have a typical spectral shape for the 4f–4f transitions of  $\text{Eu}^{3+}$ .<sup>(45,50–52)</sup> Thus, the  $\text{Eu}^{3+}$  ions were not completely reduced in the 0.5% Eu-doped glass.

Figure 6 shows the X-ray-induced scintillation decay curves of Eu-doped  $20\text{CsBr–}20\text{BaBr}_2\text{–}60\text{ZnBr}_2$  glasses. All the decay curves of Eu-doped glasses consisted of a sum of two exponential decay functions. The lifetimes of 23–25 ns and 0.36–0.41  $\mu\text{s}$  were obtained, and the faster and slower components were typical values for IRF and the 5d–4f transitions of  $\text{Eu}^{2+}$ , respectively.<sup>(38,46)</sup> Compared with the lifetimes for the PL, the lifetimes for the scintillation were slower, as well as those for other scintillators.<sup>(38,53,54)</sup>

Figure 7 shows the pulse height spectra of Eu-doped  $20\text{CsBr–}20\text{BaBr}_2\text{–}60\text{ZnBr}_2$  glasses using  $^{241}\text{Am}$   $\alpha$ -rays. The inset shows the pulse height spectra of a commercial scintillator of  $\text{Ce:Lu}_2\text{SiO}_5$  using  $^{137}\text{Cs}$   $\gamma$ -rays as the reference. To calculate the light yields, the photoabsorption peak channel of the  $\text{Ce:Lu}_2\text{SiO}_5$  scintillator corresponding to  $8700 \text{ ph/MeV} \times 0.662 \text{ MeV} = 5760 \text{ ph}$  was considered. The 0.01 and 0.05% Eu-doped glasses showed a full-energy absorption peak,

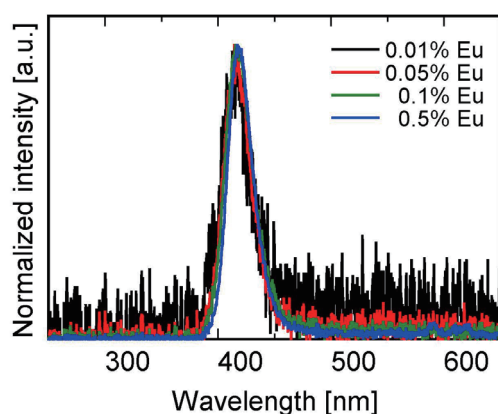


Fig. 5. (Color online) X-ray-induced scintillation spectra of Eu-doped  $20\text{CsBr–}20\text{BaBr}_2\text{–}60\text{ZnBr}_2$  glasses.

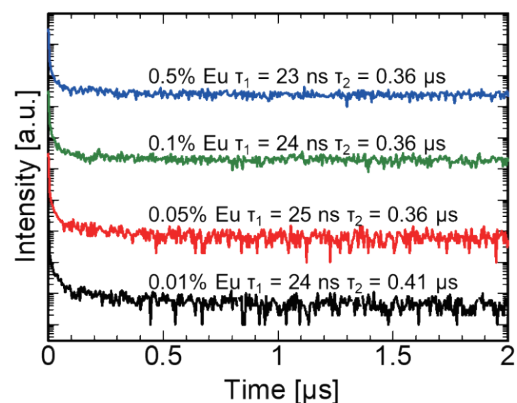


Fig. 6. (Color online) X-ray-induced scintillation decay curves of Eu-doped  $20\text{CsBr–}20\text{BaBr}_2\text{–}60\text{ZnBr}_2$  glasses.

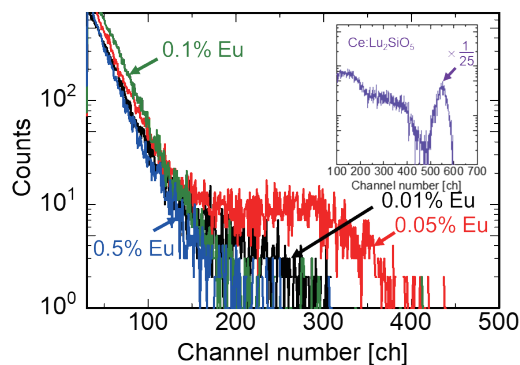


Fig. 7. (Color online) Pulse height spectra of Eu-doped  $20\text{CsBr}-20\text{BaBr}_2-60\text{ZnBr}_2$  glasses using  $^{241}\text{Am}$   $\alpha$ -rays. The inset shows the pulse height spectra of a commercial scintillator of  $\text{Ce:Lu}_2\text{SiO}_5$  using  $^{137}\text{Cs}$   $\gamma$ -rays.

and the calculated light yields of these glasses were 75 and 100 ph/5.5 MeV- $\alpha$  with a typical error of  $\pm 10\%$ , respectively. These values were comparable to those of Ce-doped  $20\text{CsCl}-20\text{BaCl}_2-60\text{ZnCl}_2$  glasses, and the light yields of these glasses were higher than those of Eu-doped  $20\text{CsCl}-20\text{BaCl}_2-60\text{ZnCl}_2$  glasses.<sup>(37,38)</sup> In the 0.1 and 0.5% Eu-doped glasses, no full-energy absorption peak was observed because of low light yields. Although the  $QY$  of 0.5% Eu-doped glasses was the highest among those of the prepared glasses, the light yields were lower than those of the 0.01 and 0.05% Eu-doped glasses; therefore, the 0.5% Eu-doped glass has the lowest energy migration efficiency from the host to the luminescence center.<sup>(55)</sup> To the best of our knowledge, this is the first report on the scintillation properties of bromide glasses.

#### 4. Conclusions

The optical and scintillation properties of Eu-doped  $20\text{CsBr}-20\text{BaBr}_2-60\text{ZnBr}_2$  glasses were investigated. As the optical properties, all the glasses showed high transmittance ( $\sim 50\%$ ). All the prepared glasses showed PL and scintillation with emission band at around 415 nm due to the  $5d-4f$  transitions of  $\text{Eu}^{2+}$ . In addition, the 0.5% Eu-doped glass showed sharp emission peaks at 590 and 610 nm attributed to the  $4f-4f$  transitions of  $\text{Eu}^{3+}$ . Among the prepared glasses, the light yield of the 0.05% Eu-doped glass was the highest (100 ph/5.5 MeV- $\alpha$ ) under  $^{241}\text{Am}$   $\alpha$ -ray irradiation. To the best of our knowledge, we have investigated the scintillation properties of bromide glasses for the first time.

#### Acknowledgments

This work was supported by Grants-in-Aid for Scientific Research B (19H03533, 21H03733, and 21H03736), Early-Career Scientists (20K20104), and JSPS Fellows (19J22091) from JSPS. The Cooperative Research Project of the Research Center for Biomedical Engineering, Nippon Sheet Glass Foundation, SEI Group CSR Foundation, TEPCO Memorial Foundation, KRF Foundation, and Murata Science Foundation are also acknowledged.

## References

- 1 S. Yamamoto, S. Okumura, N. Kato, and J. Y. Yeom: *J. Instrum.* **10** (2015) T09002.
- 2 J. Glodo, Y. Wang, R. Shawgo, C. Brecher, R. H. Hawrami, J. Tower, and K. S. Shah: *Phys. Procedia* **90** (2017) 285.
- 3 N. Kawaguchi, G. Okada, K. Fukuda, and T. Yanagida: *Nucl. Instrum. Methods Phys. Res., Sect. A* **954** (2020) 161518.
- 4 C. L. Melcher: *Nucl. Instrum. Methods Phys. Res., Sect. B* **40–41** (1989) 1214.
- 5 L. Salonen: *Sci. Total Environ.* **130–131** (1993) 23.
- 6 Y. Shirakawa: *Nucl. Instrum. Methods Phys. Res., Sect. B* **263** (2007) 58.
- 7 T. Itoh, T. Yanagida, M. Kokubun, M. Sato, R. Miyawaki, K. Makishima, T. Takashima, T. Tanaka, K. Nakazawa, T. Takahashi, N. Shimura, and H. Ishibashi: *Nucl. Instrum. Methods Phys. Res., Sect. A* **579** (2007) 239.
- 8 T. Yanagida: *Proc. Japan Acad. Ser. B* **94** (2018) 75.
- 9 P. Kantuptim, H. Fukushima, H. Kimura, D. Nakauchi, T. Kato, M. Koshimizu, N. Kawaguchi, and T. Yanagida: *Sens. Mater.* **33** (2021) 2195.
- 10 W. W. Moses: *Nucl. Instrum. Methods Phys. Res., Sect. A* **487** (2002) 123.
- 11 M. Arai, Y. Fujimoto, M. Koshimizu, H. Kimura, T. Yanagida, and K. Asai: *Mater. Res. Bull.* **120** (2019) 110589.
- 12 M. Akatsuka, H. Kimura, D. Onoda, D. Shiratori, D. Nakauchi, T. Kato, N. Kawaguchi, and T. Yanagida: *Sens. Mater.* **33** (2021) 2243.
- 13 P. Dorenbos, R. Visser, J. Andriessen, C. W. E. van Eijk, J. Valbis, and N. M. Khaidukov: *Nucl. Tracks Radiat. Meas.* **21** (1993) 101.
- 14 J. Selling, S. Schweizer, M. D. Birowosuto, and P. Dorenbos: *IEEE Trans. Nucl. Sci.* **55** (2008) 1183.
- 15 S. Matsumoto, A. Minamino, and A. Ito: *Sens. Mater.* **33** (2021) 2209.
- 16 A. Horimoto, N. Kawano, D. Nakauchi, H. Kimura, M. Akatsuka, and T. Yanagida: *Sens. Mater.* **32** (2020) 1395.
- 17 S. Emura, H. Maeda, Y. Kuroda, and T. Murata: *Jpn. J. Appl. Phys.* **32** (1993) 734.
- 18 T. Yanagida, Y. Fujimoto, M. Arai, M. Koshimizu, T. Kato, D. Nakauchi, and N. Kawaguchi: *Sens. Mater.* **32** (2020) 1351.
- 19 G. Blasse: *Chem. Mater.* **6** (1994) 1465.
- 20 T. Yanagida, Y. Fujimoto, Y. Yokota, K. Kamada, S. Yanagida, A. Yoshikawa, H. Yagi, and T. Yanagitani: *Radiat. Meas.* **46** (2011) 1503.
- 21 J. Ballato, H. Ebdorff-Heidepriem, J. Zhao, L. Petit, and J. Troles: *Fibers* **5** (2017) 11.
- 22 E. Axinte: *Mater. Des.* **32** (2011) 1717.
- 23 J. Czirr, G. MacGillivray, R. MacGillivray, and P. Seddon: *Nucl. Instrum. Methods Phys. Res., Sect. A* **424** (1999) 15.
- 24 A. Ishikawa, A. Yamazaki, K. Watanabe, S. Yoshihashi, A. Uritani, Y. Sakurai, H. Tanaka, R. Ogawara, M. Suda, and T. Hamano: *Sens. Mater.* **32** (2020) 1489.
- 25 N. Kawano, K. Shinozaki, M. Akatsuka, H. Kimura, D. Nakauchi, and T. Yanagida: *Ceram. Int.* **47** (2021) 11596.
- 26 H. Kimura, H. Masai, T. Kato, D. Nakauchi, N. Kawaguchi, and T. Yanagida: *J. Mater. Sci. Mater. Electron.* **31** (2020) 3017.
- 27 I. Kawamura, H. Kawamoto, H. Kimura, H. Komiya, Y. Fujimoto, M. Koshimizu, G. Okada, Y. Koba, R. Ogawara, M. Suda, G. Wakabayashi, T. Yanagida, and K. Asai: *Mater. Technol.* (2020) (in press). <https://doi.org/10.1080/10667857.2020.1859050>
- 28 T. Yanagida, Y. Fujimoto, H. Masai, G. Okada, T. Kato, D. Nakauchi, and N. Kawaguchi: *Sens. Mater.* **33** (2021) 2179.
- 29 A. Takaku, N. Kawano, H. Kimura, D. Nakauchi, M. Akatsuka, K. Shinozaki, and T. Yanagida: *J. Ceram. Soc. Jpn.* **128** (2020) 1024.
- 30 H. Masai, T. Ina, H. Kimura, N. Kawaguchi, and T. Yanagida: *Sens. Mater.* **33** (2021) 2155.
- 31 G. S. Henderson, D. R. Neuville, B. Cochain, and L. Cormier: *J. Non. Cryst. Solids* **355** (2009) 468.
- 32 T. Kato, S. Hirano, H. Samizo, G. Okada, N. Kawaguchi, K. Shinozaki, H. Masai, and T. Yanagida: *J. Non. Cryst. Solids* **509** (2019) 60.
- 33 T. Yanagida, N. Kawaguchi, H. Kimura, K. Shinozaki, and G. Okada: *J. Non. Cryst. Solids* **508** (2018) 46.
- 34 H. Samizo, K. Shinozaki, T. Kato, G. Okada, N. Kawaguchi, H. Masai, and T. Yanagida: *Opt. Mater.* **90** (2019) 64.

- 35 Q. Wang, B. Yang, Y. Zhang, H. Xia, T. Zhao, and H. Jiang: *J. Alloys Compd.* **581** (2013) 801.
- 36 K. Kagami, Y. Fujimoto, M. Koshimizu, T. Yanagida, K. Shinozaki, and K. Asai: *J. Mater. Sci. Mater. Electron.* **31** (2020) 4488.
- 37 G. Ito, H. Kimura, D. Shiratori, D. Nakauchi, T. Kato, N. Kawaguchi, and T. Yanagida: *Optik* **226** (2021) 165825.
- 38 G. Ito, H. Kimura, D. Shiratori, K. Hashimoto, D. Nakauchi, M. Koshimizu, T. Kato, N. Kawaguchi, and T. Yanagida: *J. Mater. Sci. Mater. Electron.* **32** (2021) 8725.
- 39 P. Egger, B. Trusch, P. Rogin, R. Giovanoli, and J. Hulliger: *Adv. Mater.* **9** (1997) 1151.
- 40 J. Lucas: *J. Non. Cryst. Solids* **80** (1986) 83.
- 41 T. Yanagida, K. Kamada, Y. Fujimoto, H. Yagi, and T. Yanagitani: *Opt. Mater.* **35** (2013) 2480.
- 42 T. Yanagida, Y. Fujimoto, T. Ito, K. Uchiyama, and K. Mori: *Appl. Phys. Express* **7** (2014) 062401.
- 43 Y. Fujimoto, T. Yanagida, M. Koshimizu, and K. Asai: *Sens. Mater.* **27** (2015) 263.
- 44 C. Li, Q. Xiao, Y. Fu, Y. Liang, C. Liu, Y. Zhuang, and L. Xia: *J. Non. Cryst. Solids* **552** (2021) 120453.
- 45 E. Malchukova and B. Boizot: *Mater. Res. Bull.* **45** (2010) 1299.
- 46 H. Kimura, T. Kato, D. Nakauchi, N. Kawaguchi, and T. Yanagida: *Sens. Mater.* **32** (2020) 1381.
- 47 C. Wang, M. Peng, N. Jiang, X. Jiang, C. Zhao, and J. Qiu: *Mater. Lett.* **61** (2007) 3608.
- 48 Z. Lian, J. Wang, Y. Lv, S. Wang, and Q. Su: *J. Alloys Compd.* **430** (2007) 257.
- 49 Q. Zhang, X. Liu, Y. Qiao, B. Qian, G. Dong, J. Ruan, Q. Zhou, J. Qiu, and D. Chen: *Opt. Mater.* **32** (2010) 427.
- 50 Y. Isokawa, H. Kimura, T. Kato, N. Kawaguchi, and T. Yanagida: *Opt. Mater.* **90** (2019) 187.
- 51 K. Shinozaki, T. Honma, and T. Komatsu: *Opt. Mater.* **36** (2014) 1384.
- 52 N. Kawano, H. Kimura, A. Horimoto, K. Shinozaki, and T. Yanagida: *J. Mater. Sci. Mater. Electron.* **30** (2019) 11468.
- 53 H. Kimura, F. Nakamura, T. Kato, D. Nakauchi, N. Kawano, G. Okada, N. Kawaguchi, and T. Yanagida: *Optik* **157** (2018) 421.
- 54 F. Nakamura, T. Kato, G. Okada, N. Kawaguchi, K. Fukuda, and T. Yanagida: *J. Alloys Compd.* **726** (2017) 67.
- 55 D. J. Robbins: *J. Electrochem. Soc.* **127** (1980) 2694.